

A Broadband Dual-polarized Antenna for 2G/3G/4G/5G Base Station Applications

Ya-Li Chen¹, Yao-Zong Sui¹, Zhi-Qun Yang², Xiao-Yun Qu², and Wei-Hua Zong^{1*}

¹ School of Electronics and Information
Qingdao University, Qingdao, 266000, China
*weihuazong@126.com

² Shandong Institute of Space Electronic Technology
Yantai, 264003, China

Abstract — This paper presents a novel broadband base station antenna element covering 2G/3G/4G/5G bands. The proposed antenna consists of a dual-dipole radiator and an open-box shaped reflector. The main radiating portion of each dipole arm is designed with a dual-hexagon shape to improve bandwidth. Four small hexagonal-shaped parasitic patches are adopted to further decrease the reflection coefficient. Dual polarization is excited by placing two dipoles orthogonally. The open-box shaped reflector derives from a planar metal plate with four inverted L-shaped edges which are arranged below the radiator to enhance the antenna gain and reduce the half power bandwidth (HPBW) in 3.3-3.8 GHz. The prototype has been fabricated and measured with bandwidth of 1.68-3.8 GHz, coupling below -20 dB, stable HPBW with $65^\circ \pm 5^\circ$ and average gain of 8.5 dBi. The values of the cross-polarization discrimination (XPD) are better than 20 dB at the boresight and 10 dB within $\pm 60^\circ$ directions. The proposed antenna has a small overall size of $145 \times 145 \times 35.6$ mm³.

Index Terms — 5G antenna, base station antenna, broadband antenna, dual-polarized antenna.

I. INTRODUCTION

The fifth-generation (5G) communication working at the FR1 band (0.45-6 GHz) has been commercially launched in many countries to provide high-speed data transmission and high-quality network link. There is an urgent need for base station antennas covering 5G FR1 band. The frequency bands of 2G/3G/4G are appealing to be included in the a 5G antenna covering 1.71-3.8 GHz frequency band [1] to save the space volume of a base station system. Dual polarization is also required for a base station antenna to increase channel capacity and decrease channel fading influence.

Plenty of researches on base station antenna have been performed over the last few years. To obtain dual polarization, adopting double orthogonal dipoles is an

effective method [1-11]. Antenna with single patch can also achieve dual polarization by using orthogonal feeding lines [12] or slots [13-14].

To improve antenna bandwidth, a number of techniques have been proposed. In [3], a filter-based matching circuit is adopted to feed full-wavelength dipoles. In [4], parasitic patches are arranged on top of four-loop radiators for bandwidth enhancement. Wide bandwidth can be also achieved by designing dipole arm's shape and improving coupling between adjacent arms [5-6]. In [7], double annular disks and gradient strips are adopted for the bandwidth enhancement. In [15], a stepped-impedance feeding structure combining with a T-shaped patch is used to excite multiple resonances. Microstrip balun is adopted in [16] to improve bandwidth. It is still challenging to design a broadband base station antenna covering 2G/3G/4G/5G bands with dual polarization and stable half power bandwidth (HPBW).

In this paper, a planar base station antenna covering 2G/3G/4G/5G bands of 1.71-3.8GHz is proposed. The radiator consists of a pair of double-hexagon dipoles and four small hexagonal parasitic patches printed on double layers of the substrate orthogonally to achieve wide bandwidth and dual polarization. Four inverted L-shaped edges are added to a planar reflector enhance the antenna gain and reduce the HPBW.

II. ANTENNA CONFIGURATION

The configuration of the dual-polarized antenna is illustrated in Fig. 1. The proposed antenna consists of a radiator and a reflector. The radiator includes four main patches with double-hexagon shape (MP₁₁, MP₁₂, MP₂₁ and MP₂₂) and four small parasitic patches (PP₁, PP₂, PP₃ and PP₄). The main patches of MP₁₁ and MP₁₂ form a planar dipole with +45° polarization, and MP₂₁ and MP₂₂ form another one with -45° polarization. Each main patch consists of a larger hexagonal patch embedded with a smaller one. The larger hexagonal patch is etched with a polygonal slot to avoid overlapping with the inner

smaller one. As shown in Fig. 1, MP_{21} , PP_1 , PP_2 and PP_3 are printed on the top layer of a FR-4 dielectric substrate, and MP_{11} , MP_{12} , MP_{22} and PP_4 are printed on its bottom layer. The FR-4 substrate has a relative permittivity of 4.4 and a dielectric loss tangent of 0.02.

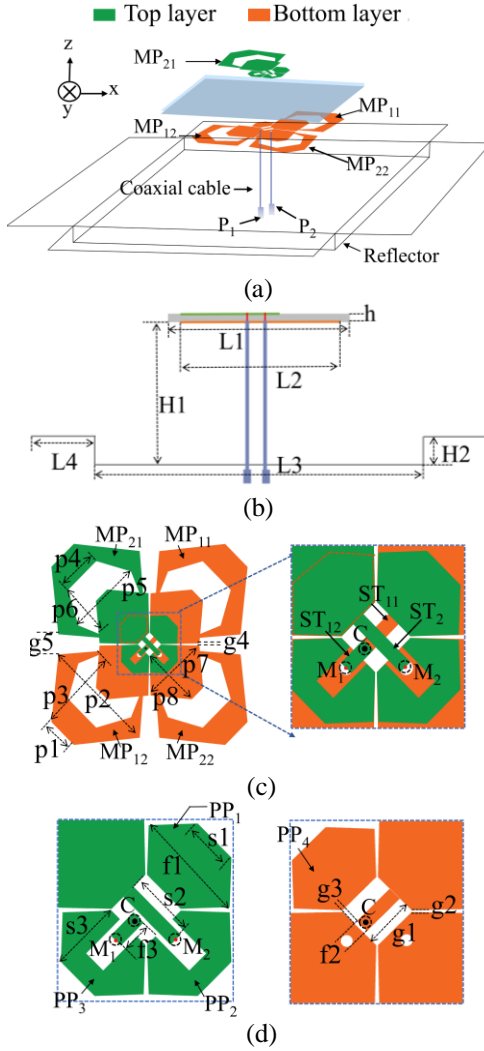


Fig. 1 Configuration of the proposed antenna: (a) 3-D view, (b) front view, (c) double layers of the radiator, and (d) the center portion of each layer in detail.

The two planar dipoles are fed at M_1 and M_2 points through three feeding strips of ST_{11} , ST_{12} and ST_2 . To avoid the overlap among the feeding strips, ST_{12} and ST_2 are printed on the top layer, and ST_{11} is printed on the bottom layer. MP_{11} and MP_{12} are both on the bottom layer and fed at M_1 through ST_{12} and ST_{11} . ST_{12} starts at point M_1 on the top layer, and connects to ST_{11} at point C via a metalized hole, then ST_{11} connects to MP_{11} on the bottom layer. MP_{21} and MP_{22} are on different layers and fed at M_2 through ST_2 . Coaxial cables are adopted to transform electrical signals. The inner conductors of the

two coaxial cables are soldered with the end of ST_{12} and ST_2 at M_1 and M_2 points on the top layer, respectively. The outer conductors are soldered with MP_{12} and MP_{22} on the bottom layer, respectively.

Four inverted L-shaped edges are added to a planar reflector to enhance the gain and satisfy the HPBW requirement at the frequency band of 3.3-3.8 GHz. All of the details will be discussed in Section III. The proposed antenna was simulated and optimized by HFSS 15.0. Table 1 lists the optimized geometric dimension.

Table 1: Dimensions of the proposed antenna

Par.	Value (mm)	Par.	Value (mm)	Par.	Value (mm)
L1	55	f3	2.7	p1	8
L2	49.5	g1	4.2	p2	29
L3	95	g2	0.3	p3	19.7
L4	25	g3	0.5	p4	10
h	0.6	g4	0.7	p5	18.8
H1	35	g5	5	p6	12.7
H2	10	s1	4	p7	17.4
f1	5.6	s2	17.4	p8	15
f2	1.2	s3	6		

III. ANTENNA ANALYSIS

A. Radiation element analysis

The evolution of the radiator is depicted in Fig. 2 and their reflection coefficients are shown in Fig. 3. Ant. I is a dual-dipole antenna with hexagonal shaped patches. As shown in Fig. 3, Ant. I has better reflection coefficient at lower band but worse at frequencies above 3.2 GHz. The antenna bandwidth can be improved by optimizing the gap between each arm of the two dipoles [5-6]. Different from the published method, a smaller hexagonal patch is embedded into each larger hexagonal patch to get a tapered gap between each dipole arm. Each larger hexagon patch is etched with a polygonal slot to avoid overlapping with the smaller hexagonal patch which results in Ant. II. A new resonance is excited for Ant. II which results in improved -10 dB bandwidth of 1.59-4.34 GHz. However, the reflection coefficient is near -10 dB at 3.3-3.7 GHz. Considering fabrication errors, it might exceed -10 dB at these frequencies. Based on Ant. II, the proposed antenna is obtained by adding of a parasitic patch on the opposite layer of each main patch. As shown Fig. 3, the third resonance shifts to the lower frequency and the reflection coefficient decreases much in the 1.7-3.8 GHz band. The proposed antenna has a wide -10 dB bandwidth of 1.64-4.2 GHz, and -15 dB band of 1.71-4 GHz.

Current distributions of the proposed antenna and Ant. II at 3.6 GHz are plotted in Fig. 4 to illustrate the working mechanism of the parasitic patches. As shown in the figure, the parasitic patches induce more current distributing on the boundary of the main patches which

improve the impedance matching.

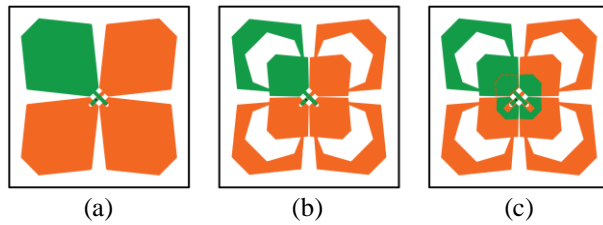


Fig. 2. Evolution of the radiator: (a) Ant. I, (b) Ant. II, and (c) the proposed antenna.

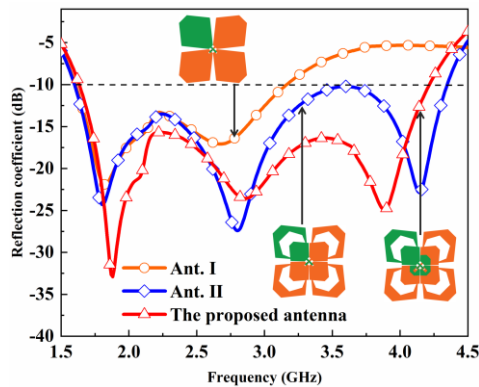


Fig. 3. Reflection coefficient of three antennas.

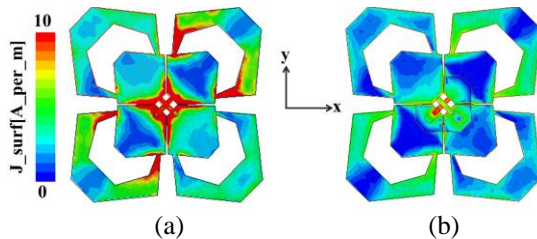


Fig. 4. Current distributions at 3.6 GHz: (a) Ant. II and (b) the proposed antenna.

The gap size between two adjacent arms has a strong effect on the reflection coefficient. The influence of g_2 and g_4 is illustrated in Fig. 5 and Fig. 6, respectively. As shown in Fig. 5, changing of g_2 has much influence on reflection coefficient at 3.3-3.8 GHz. At these frequencies, the reflection coefficient reduces dramatically with the decrease of g_2 . Considering fabrication error, g_2 cannot be too small. As shown in Fig. 6, in the frequency range of 3-4 GHz, the reflection coefficient becomes larger with the increase of g_4 , and smaller in the frequency range of 2-2.7 GHz. The optimized bandwidth is obtained with $g_2=0.5$ mm and $g_4=5$ mm.

B. Reflector analysis

In a mobile communication system, the base station antenna is required with a $65\pm 5^\circ$ HPBW to cover 120°

sector. It is challenging to design a reflector keeping stable patterns in the whole band of 1.71-3.8 GHz. The antenna with a planar reflector proposed in [6] has a $65^\circ \pm 5^\circ$ HPBW at 1.7-2.7 GHz and 95° at 3.4-3.6 GHz. The open-box shaped reflector proposed in this paper provides satisfied HPBW at 1.7-3.8 GHz.

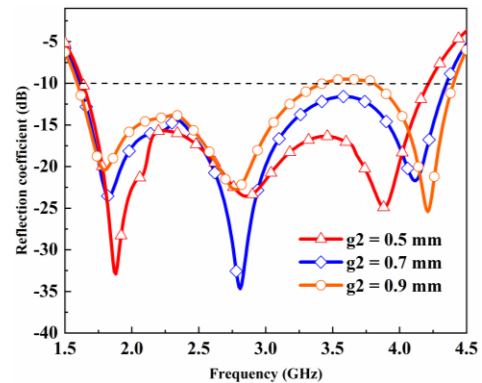


Fig. 5. Reflection coefficient versus g_2 .

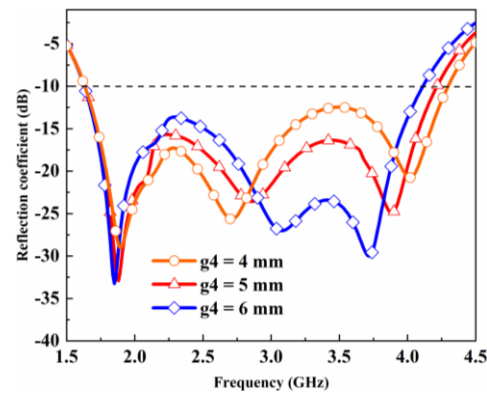


Fig. 6. Reflection coefficient versus g_4 .

The distance between the radiator and the reflector is crucial to a base station antenna's radiation pattern. It also affects the reflection coefficient. A planar reflector is arranged under the radiator with the distance of H_1 to study the influence of the distance. Figure 7 and Fig. 8 show the influence of H_1 on radiation pattern. As shown in the figures, narrower HPBW and higher gain are obtained with the decrease of H_1 at frequencies above 2.3 GHz. Figure 9 shows (the) reflection coefficient with different H_1 . As shown in the figure, the reflection coefficient at lower band becomes worse with the decrease of H_1 owing to the inductive current on the ground plane. The distance between an antenna radiator and a planar reflector is often adopted as a quarter wavelength to balance the radiation pattern and the bandwidth. Therefore, $H_1=35$ mm is suitable for lower frequencies around 2.1 GHz, and $H_1=25$ mm is suitable for the upper band around 3 GHz. The proposed open-box shaped reflector meets the lower frequencies'

requirement with the bottom planar reflector at 35 mm under the radiator, and the four inverted-L shaped metal edges increasing 10 mm height meet the upper frequencies. Figure 10 gives comparison of HPBW and realized gain of the proposed radiator with a planar reflector, a box-shaped reflector, and the proposed open-box shaped reflector. As shown in the figure, with adding of four edges between the radiator and reflector, the HPBW decreases and the gain increases. The proposed reflector provides $65^\circ \pm 5^\circ$ HPBW and higher than 8 dBi gain in 1.71-3.8 GHz.

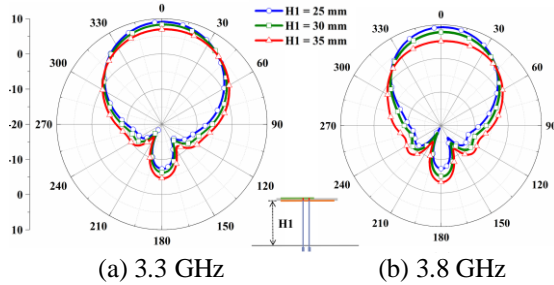


Fig. 7. Radiation pattern of the proposed radiator with a planar reflector with different H1.

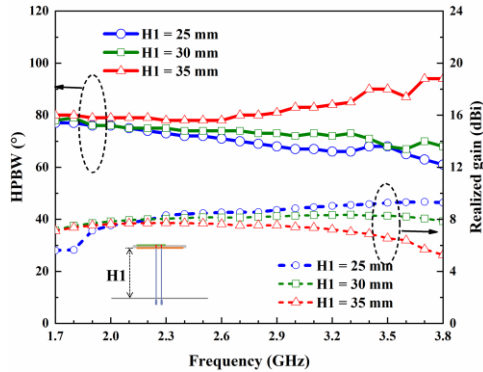


Fig. 8. HPBW and realized gain of the proposed radiator with a planar reflector varying with different H1.

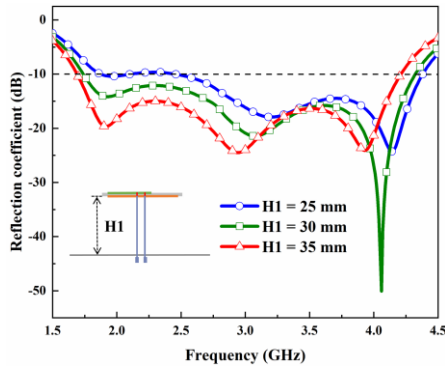


Fig. 9. Reflection coefficient of the proposed radiator with a planar reflector varying with H1.

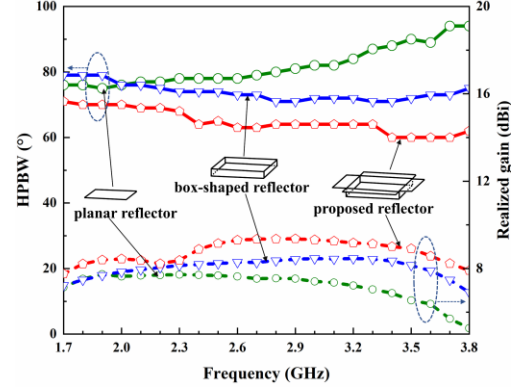


Fig. 10. HPBW and realized gain of three reflectors.

C. Current distribution

Current distributions on the radiator at 1.8, 2.5 and 3.5 GHz are shown in Fig. 11. As shown in the figure, when P_1 is excited, the current mainly distributes on the $+45^\circ$ polarization dipole and points to $+45^\circ$ direction. There are also currents distributing on the cross dipole which are induced by coupling. The path of coupling currents forms closed loops resulting in weak radiation. Therefore, $+45^\circ$ polarization is obtained. When P_2 is excited, -45° polarization is achieved. Although current distributions differ much at different frequencies, it can be seen that strong currents distribute at the gap edges between two adjacent arms at any frequency. It means that the gap size is crucial for impedance matching.

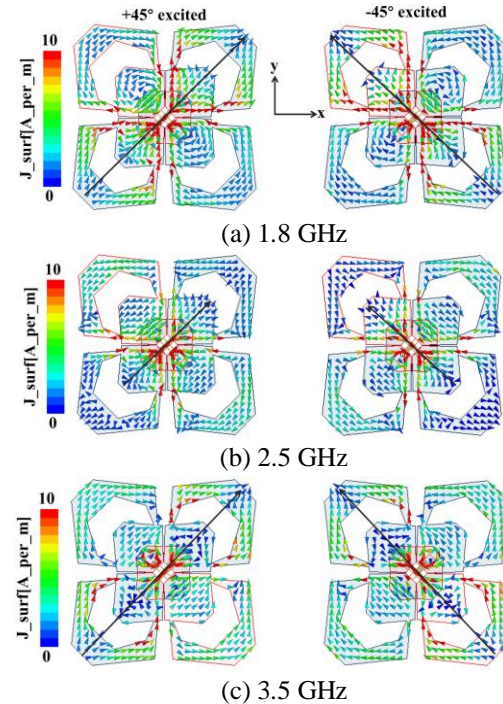


Fig. 11. Current distributions on the radiator.

IV. RESULTS AND DISCUSSION

The prototype of the proposed antenna has been fabricated and measured. Figure 12 shows photographs of the fabricated antenna. The comparison of the simulated and measured S-parameters is shown in Fig. 13 and Fig. 14. There is an obvious discrepancy between simulation and measurement. The simulated -10 dB bandwidth is 1.62-4.21 GHz, and -15 dB bandwidth is 1.71-4 GHz. The measured reflection coefficient is higher than -11 dB with -10 dB bandwidth of 1.68-3.8 GHz. The simulated coupling is lower than -26 dB in 1.5-4.4 GHz. The measured coupling is higher than simulation in 1.6-3.2 GHz, and lower than -20 dB in the whole band. The discrepancy between simulation and measurement might come from fabrication errors, coaxial cable losses and soldering point losses.

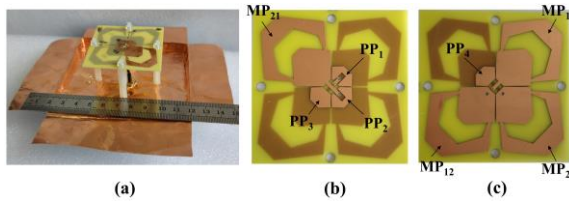


Fig. 12. Photographs of the fabricated antenna: (a) the whole antenna, (b) top layer of the radiator, and (c) bottom layer of the radiator.

Due to geometric symmetry of the proposed antenna, only the $+45^\circ$ polarization results are shown in Fig. 15 and Fig. 16. Figure 15 displays gain and total efficiency. It can be observed that the average simulated gain is 8.8 dBi agreeing with the measured one of 8.5 dBi. The simulated efficiency is a bit lower than the simulation with values higher than 80% in the whole band. Figure 16 presents radiation patterns of the horizontal plane (i.e., xOz) at 1.78, 2.18, 2.48, 2.68, 3.48 and 3.68 GHz. Both the simulated and measured results show that the proposed antenna has a stable HPBW around $65^\circ \pm 5^\circ$ at the whole operational band. The values of the cross-polarization discrimination (XPD) are better than 20 dB at the boresight and 10 dB within $\pm 60^\circ$ directions.

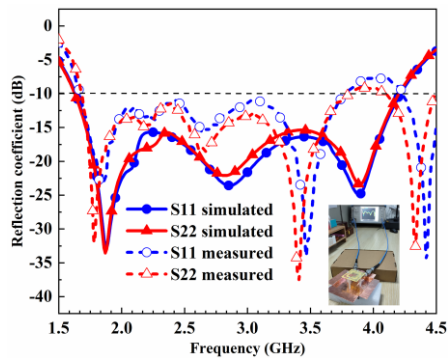


Fig. 13. Simulated and measured reflection coefficients.

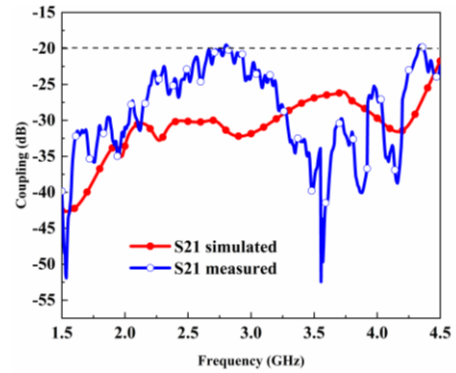


Fig. 14. Simulated and measured coupling.

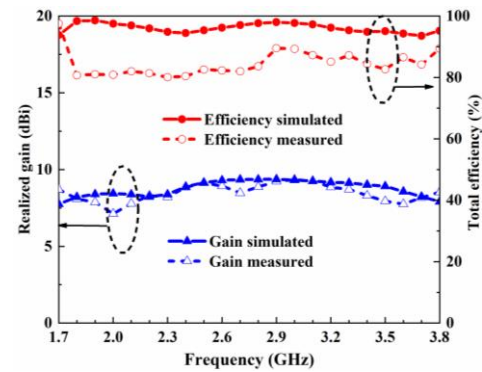


Fig. 15. Gain and total efficiency with $+45^\circ$ excited.

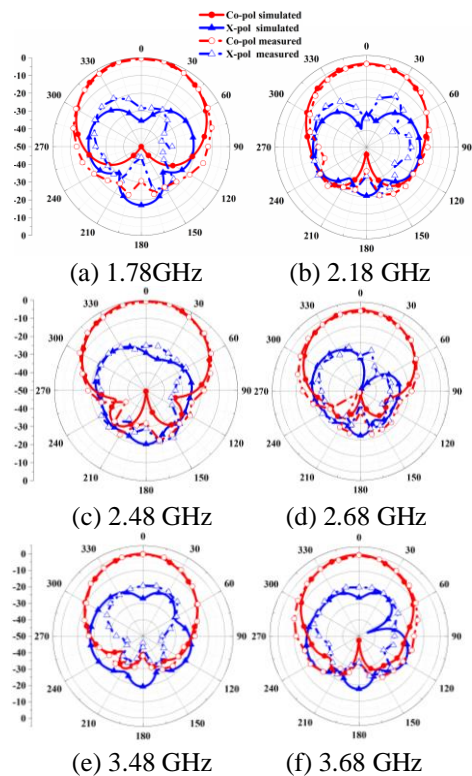


Fig. 16. Radiation patterns with $+45^\circ$ excited.

Table 2 shows the comparison of the proposed antenna with published papers. The proposed antenna has wider bandwidth than [2], [4], [12], better HPBW and higher gain than [6].

Table 2: Comparison of the proposed antenna with published literatures

Ref.	Size (mm ³)/ Size (λ_L^3)	VS WR	BW (GHz)	Coup. (dB)	Gain (dBi)	HP BW
[3]	160×160×41.8/ 0.87×0.87×0.23	2	1.63-3.71	-28	/	58°-64°
[4]	130×130×25.5/ 0.96×0.96×0.19	1.5	2.21-3.63	-30	8.3	60°-71°
[6]	145×145×36/ 0.81×0.81×0.2	1.5	1.68-3.7	-28	*8.6 **6.5	*61°-71° **95°
[12]	75×75×13.1/ 0.7×0.7×0.11	2	2.78-4.4	-28	8.95	56°-65°
Pro.	145×145×35.6/ 0.81×0.81×0.2	2	1.68-3.8	-20	8.5	60°-70°

* is at 1.7-2.7 GHz, ** is at 3.4-3.6 GHz.

λ_L is the free space wavelength at the lowest operational frequency.

V. CONCLUSION

A dual-polarized base station antenna has been presented in this paper. By adjusting the gap between two dipoles' arms, the proposed antenna has achieved a broad bandwidth of 1.68-3.8 GHz with coupling below -20 dB. The overall volume of the proposed antenna is 145×145×35.6 mm³. It has an average gain of 8.5 dBi, stable HPBW around 65°± 5° in the horizontal plane and XPD better than 10 dB in the whole -10 dB band. The proposed antenna is a promising and economical candidate of 2G/3G/4G/5G communication systems.

ACKNOWLEDGMENT

This work was supported by the Natural Science Foundation of Shandong Province, China (No. ZR2020MF023).

REFERENCES

- [1] Q. Wu, P. Y. Liang, and X. M. Chen. "A broadband $\pm 45^\circ$ dual-polarized multiple-input multiple-output antenna for 5G base stations with extra decoupling elements," *Journal of Communications and Information Networks*, vol. 3, no. 1, pp. 31-37, Mar. 2018.
- [2] S. X. Ta, D. M. Nguyen, K. K. Nguyen, C. D. Ngoc, and N. N. Trong, "Wideband differentially fed dual-polarized antenna for existing and sub-6 GHz 5G communications," *IEEE Antennas and Wireless Propagation Letters*, vol. 19, no. 12, pp. 2033-2037, Dec. 2020.
- [3] C. Ding, H. Sun, H. Zhu, and Y. Jay Guo, "Achieving wider bandwidth with full-wavelength dipoles for 5G base stations," *IEEE Transactions on Antennas and Propagation*, vol. 68, no. 2, pp. 1119-1127, Feb. 2020.
- [4] B. Wang, C. C. Zhu, C. Y. Liao, W. Luo, B. Yin, and P. Wang, "Broadband dual-polarized dipole antenna for LTE/5G base station applications," *Electromagnetics*, vol. 40, no. 1, pp. 13-22, Nov. 2019.
- [5] D. Zheng and Q. Chu, "A wideband dual-polarized antenna with two independently controllable resonant modes and its array for base-station applications," *IEEE Antennas and Wireless Propagation Letters*, vol. 16, pp. 2014-2017, July 2017.
- [6] Y. Zhang, Y. Zhang, D. Li, K. Liu, and Y. Fan, "Ultra-wideband dual-polarized antenna with three resonant modes for 2G/3G/4G/5G communication systems," *IEEE Access*, vol. 7, pp. 43214-43221, Apr. 2019.
- [7] Z. Li, J. Han, Y. Mu, X. Gao, and L. Li, "Dual-band dual-polarized base station antenna with a notch band for 2/3/4/5G communication systems," *IEEE Antennas and Wireless Propagation Letters*, vol. 19, no. 12, pp. 2462-2466, Dec. 2020.
- [8] B. Feng, L. Li, K. L. Chung, and Y. Li, "Wideband widebeam dual circularly polarized magnetolectric dipole antenna/array with meta-columns loading for 5G and beyond," *IEEE Transactions on Antennas and Propagation*, vol. 69, no. 1, pp. 219-228, Jan. 2021.
- [9] B. S. Qiu, S. Y. Luo, and Y. S. Li, "A broadband dual-polarized antenna for Sub-6 GHz base station application," *2020 IEEE 3rd International Conference on Electronic Information and Communication Technology (ICEICT)*, pp. 273-275, Nov. 2020.
- [10] H. Zhai, J. Zhang, Y. Zang, Q. Gao, and C. Liang, "An LTE base-station magnetolectric dipole antenna with anti-interference characteristics and its MIMO system application," *IEEE Antennas and Wireless Propagation Letters*, vol. 14, pp. 906-909, Apr. 2015.
- [11] P. Chen, L. H. Wang, and T. Y. Ding, "A dual-polarized sakura-shaped base station antenna for 5G communications," *Applied Computational Electromagnetics Society Journal*, vol. 35, no. 5, pp. 567-571, May 2020.
- [12] M. Ciydem and E. A. Miran, "Dual-polarization wideband sub-6 GHz suspended patch antenna for 5G base station," *IEEE Antennas and Wireless Propagation Letters*, vol. 19, no. 7, pp. 1142-1146, July 2020.
- [13] R. Lian, Z. Wang, Y. Yin, J. Wu, and X. Song, "Design of a low-profile dual-polarized stepped slot antenna array for base station," *IEEE Antennas and Wireless Propagation Letters*, vol. 15, pp. 362-365, Feb. 2016.
- [14] Y. Liu, S. Wang, X. Wang, and Y. Jia, "A differentially fed dual-polarized slot antenna with high isolation and low profile for base station application," *IEEE Antennas and Wireless Propagation Letters*, vol. 18, no. 2, pp. 303-307, Feb.

2019.

- [15] Q. Hua, Y. Huang, S. Y. Song, M. O. Akinsolu, B. Liu, T. Y. Jia, Q. Xu, and A. Alieldin, "A novel compact quadruple-band indoor base station antenna for 2G/3G/4G/5G systems," *IEEE Access*, vol. 7, pp. 151350-151358. Oct. 2019.
- [16] G. Gopal and A. Thangakalai, "Cross dipole antenna for 4G and sub-6 GHz 5G base station applications," *Applied Computational Electromagnetics Society Journal*, vol. 35, no. 1, pp. 16-22, Jan. 2020.



Qingdao, China. Her current research interest is in base station antennas.

Ya-Li Chen was born in Neijiang, Sichuan, China, in 1997. She received the B.S. degree in Information Engineering from Hangzhou Dianzi University, Hangzhou, China, in 2019. She is currently pursuing the M.S. degree in Signal and Information Processing in Qingdao University,



present, the research direction is antenna design.

Yao-Zong Sui was born in Shouguang, Shandong Province, China in 1996. In 2018, he graduated from the Electronic Information of Qingdao University. In 2020, He entered Qingdao University to pursue a master's degree in Signal and Information Processing. At



Corporation, Yantai, China, as a Senior Engineer. His research interest is signal processing and communication.

Zhi-Qun Yang received the Ph.D. degree in Communication and Information System from Nanjing University of Technology, Nanjing, Jiangsu Province, China, in 2003. He is with Shandong Institute of Space Electronic Technology, China Aerospace Science and Technology



Nanjing, Jiangsu Province, China, in 1990. She is with Shandong Institute of Space Electronic Technology, Yantai, China, as a Senior Engineer. Her research interest is antenna design.

Xiao-Yun Qu was born in Yantai City, Shandong Province, China, in 1974. She received the B.S. in Applied Mathematics from Yantai University, in 1996, M.S. degree in Electromagnetic Fields and Microwave Technology from Nanjing Electronics Research Center,



Nanjing, Jiangsu Province, China, in 2000, and the Ph.D. degree in Electromagnetic Fields and microwave Technology from Xidian University, Xian, Shanxi Province, China, in 2004. In 2004, she joined Qingdao University, Qingdao, Shandong Province, China as a Lecturer. Since 2005, she has been an Associate Professor in Qingdao University. From February 2010 to August, she was a Visiting Scholar Assistant with Electrical and Computation Engineering Department, National University of Singapore. Her research interests include antenna design and electromagnetic material measurement.

Wei-Hua Zong was born in Penglai City, Shandong Province, China, in 1975. She received the B.S. in Applied Mathematics from Yantai University, in 1997, M.S. degree in Electromagnetic Fields and Microwave Technology from Nanjing Electronics Research Center,